# Modeling the Process of Drying Stationary Objects inside a Tumble Dryer Using COMSOL Multiphysics

T. Zeineldin
Department of Automatic Control and Mechatronics, University of Paderborn, NRW, Germany
Pohlweg 98, D-33098 Paderborn, NRW, Germany – Tarek.Zeineldin@rtm.upb.de

**Abstract:** Temperature and residual moisture content of stationary Textile in a home Tumble dryer are simulated in a 2D model with COMSOL Multiphysics. Moisture immigration to the textile surface is modeled in the form of capillary flow and vapor diffusion while heat transfer in the form of conduction and energy lost due to phase change (evaporation). The drying air energy, mass and momentum transport were coupled to the textile model simulation but not included in the model validation. The simulation results show good agreement with our measurements.

**Keywords:** drying, temperature, moisture content.

## 1. Introduction

Tumble Dryers are one of the most energy consuming home appliances. This energy consumption level is even elevated by the fact that during the drying process parts of the goods are not completely dry while other parts are over dried (having less moisture content than the room quality). This causes a prolongation of the process. Air flow through the dryer drum as well as many other factors dramatically affects the process efficiency. The model we present in this paper serves as a first step to better understanding and enhancing such factors in order to increase the process efficiency.

The modeling procedure implemented in this paper is strongly based on the mathematical model of drying processes adapted by Chen and Pei[1]. However we have taken some further simplifications in order to ease the modeling in COMSOL yet containing the error in our region of tolerance:

1. The moisture content is all free.
2. Neglecting the drying front movement.

In this paper we describe two models. The first model: **Model A** couples energy and mass transport in and out of the textile during the drying process where the air temperature and relative humidity are predetermined (from the measurements). In the second model: **Model B**, the air temperature and quality are modeled. Due to the large surface area of the drum and the limited computer power available, we could not run the simulation with the required mesh resolution for Model B. Therefore a smaller area was rather implemented and the model validation was limited to Model A.

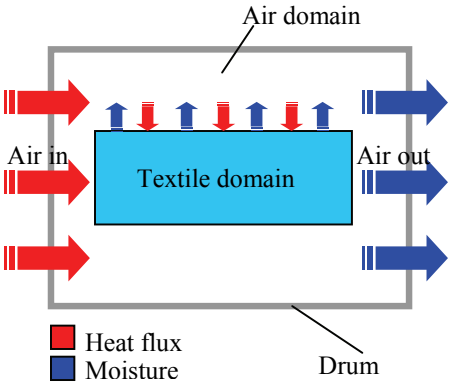


**Figure 1**. Problem schematic

## 2. Governing Equations

### Laundry Energy Transport

In drying processes, temperature is the driving force. The higher the air temperature, the more energy can be transported to the textile surface:

$$k_t \cdot \nabla T = \alpha \cdot (T_a - T) + \rho_w \cdot D_w \cdot \nabla X \cdot \Delta h_v$$

Energy Boundary Equation (1)

Here $k_t$, T, X, $T_a$, $\rho_w$, X and $\Delta h_v$ are the textile heat conductivity, temperature, moisture content, air temperature, water density and the enthalpy of evaporation respectively. The capillary conductivity $D_w$ and the coefficient of heat transfer $\alpha$ are functions of the residual moisture content. We will shortly come to these functions in more detail.

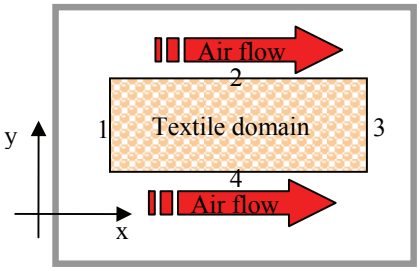


**Figure 2**. Textile domain and boundaries

Energy continues to flow from the surface to the inside of the textile due to temperature differences:

$$\rho_t \cdot c_{p,t} \cdot \frac{\partial T}{\partial t} = \nabla(k_t \cdot \nabla T) - \dot{m}_{ev} \cdot \Delta h_v \qquad (2)$$

Energy Subdomain Equation

Where ρ, $c_p$ and t are the density, specific heat capacity and time. The second term on the right hand side represents the energy lost with the portion of moisture that evaporates, where $m_{ev}$ is the evaporated mass rate per unit volume.

## Laundry Mass Transport

The Energy passing into the textile helps the moisture overcome the binding forces, raises the vapor pressure and drives the moisture out to the surface:

$$\rho_w \cdot \frac{\partial X}{\partial t} = \rho_w \cdot \nabla(D_w \cdot \nabla X) - \dot{m}_{ev} \qquad (3)$$

Mass Subdomain Equation

$D_w$ is a function of the residual moisture content. This function has two formulas depending on the type of water migrating. As we assumed that all is free water the following formula is used:

$$D_w = (1.604 \cdot T - 394.3) \cdot \beta_1 \cdot K_0 \cdot \left(\frac{X - X_{ms}}{X_s - X_{ms}}\right)^3 \qquad (4)$$

Here $\beta_1$, $K_0$, $X_{ms}$, $X_s$ are a constant, single phase permeability, maximum sorptive moisture content and saturation moisture content respectively.

This moisture is then carried by the dry air off the textile surface:

$$\frac{D_v \cdot M_w}{R \cdot T} \cdot \nabla p_{v,t} + \rho_w \cdot D_w \cdot \nabla X = \frac{\beta \cdot M_w}{R} \cdot \left(\frac{p_{v,a}}{T_a} - \frac{p_{v,t}}{T}\right) \qquad (5)$$

Mass Boundary Equation

The first term on the left hand side of the equation accounts for the vapor transfer from/in the inside of the laundry depending on the vapor pressure ($p_v$) gradient, where $D_v$ is the vapor diffusion coefficient and $M_w$ is the molecular weight of water. The mass transfer coefficient β is a function of the moisture content:

$$\beta = \beta_0 \cdot \left(\eta_m + (1 - \eta_m) \cdot \frac{X - X_{ms}}{X_c - X_{ms}}\right) \qquad (6)$$

As previously mentioned the heat transfer coefficient is also a function of the residual moisture content:

$$\alpha = \alpha_0 \cdot \left(\eta_h + (1 - \eta_h) \cdot \frac{X - X_{ms}}{X_c - X_{ms}}\right) \qquad (7)$$

$\alpha_0$, $\beta_0$, $\eta_m$, $\eta_h$ are constants determined experimentally while $X_c$ is the critical moisture content. The formulas for α and β are only valid in the following range:

$$X_{ms} < X < X_c$$

Otherwise, experimental values are applied.

## Air Energy and Mass Transport

The air governing equations are a bit different from textile as an additional convection term appears due to the velocity of air:

$$\rho_a \cdot c_{p,a} \frac{\partial T}{\partial t} = \nabla(k_a \cdot \nabla T) - \rho_a \cdot c_{p,a} \cdot u \cdot \nabla T$$

Energy Subdomain Equation (8)

$$\frac{\partial X}{\partial t} = \nabla(D_v \cdot \nabla X) - u \cdot \nabla X \qquad (9)$$

Mass Subdomain Equation

The second term on the right hand side of equations 8 and 9 resembles the convective heat due to air velocity, where u is the air velocity.

As shown in Figure (3), air has 8 boundaries:

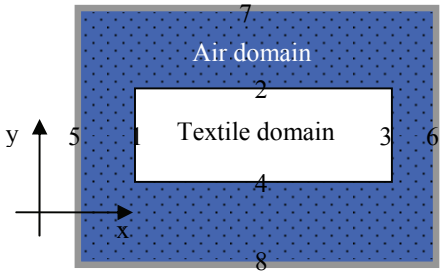


**Figure 3**. Air domain and boundaries

- Four Boundaries surrounding the textile; 1,2,3 and 4:

$$k_a \cdot \nabla T = \alpha \cdot (T - T_t) + \rho_a \cdot c_{p,a} \cdot v \cdot T \quad (10)$$

$$\rho_v \cdot D_v \cdot \nabla X - u \cdot X = \frac{\beta \cdot M_w}{R} \cdot \left(\frac{p_{v,a}}{T} - \frac{p_{v,t}}{T_t}\right) - \frac{D_v \cdot M_w}{R \cdot T_t} \cdot \nabla p_{v,t} \quad (11)$$

- Inlet Boundary; 5:

$$T = T_0 \quad (12)$$

$$X = X_0 \quad (13)$$

- Outlet Boundary; 6 (Convective flux):

$$k_a \cdot \nabla T = 0 \quad (14)$$

$$D_v \cdot \nabla X = 0 \quad (15)$$

- Two wall boundaries; 7 and 8 (Insulation):

$$k_a \cdot \nabla T - \rho_a \cdot c_{p,a} \cdot u \cdot T = 0 \quad (16)$$

$$D_v \cdot \nabla X - u \cdot X = 0 \quad (17)$$

**Air Momentum Transport**

Due to the heat transfer and the variation in temperature and density we have chosen the weakly compressible flow to model the air momentum transport:

$$\rho_a \frac{\partial u}{\partial t} + \rho_a \cdot u \cdot \nabla u = \nabla T + F \quad (18)$$

$$\frac{\partial \rho_a}{\partial T} + \nabla(\rho_a \cdot u) = 0 \quad (19)$$

Momentum Subdomain Equations

Here T and F are the total force per area and the volume force.

The boundary conditions at the textile; 1,2,3 and 4 and the walls; 7 and 8 are the same (no slip):

$$u = 0 \quad (20)$$

At the inlet; 5:

$$u = u_0 \quad (21)$$

And at the exit; 6:

$$p = p_0 \quad (22)$$

Where p is the pressure.

## 3. Results and Discussion

Typical tumble dryer cycles have three phases. The cycle starts with an increasing air drum inlet temperature. In the second phase, the inlet temperature stays almost constant. At the end, the cooling phase follows where the textile is brought to the room temperature (Figure 4). In all three phases the air enters with a low vapor pressure to create a higher concentration gradient at the textile surface (Figure 5).

Experiments were carried on 7cm thick layers of cotton textile. The initial moisture content was 0.6 Kg water/ Kg cotton. Temperatures at the drum inlet and the inside of the textile (Figure 6) were measured. The relative humidity at the drum inlet was also measured in order to generate the vapor pressure curves in Figure 5. The apparatus used was a 2.9KW commercial condenser dryer, with a process air volume rate of 120 $m^3$/hr.

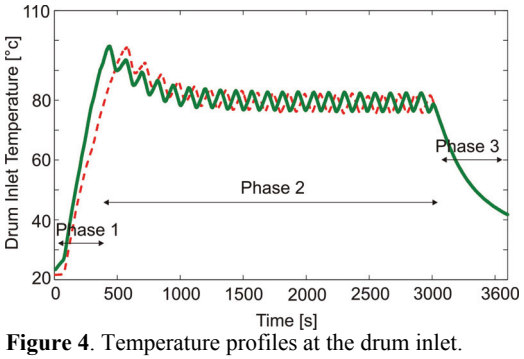


**Figure 4**. Temperature profiles at the drum inlet.

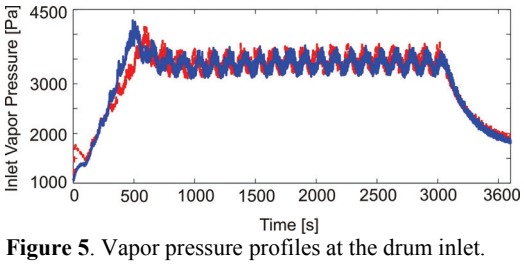


**Figure 5**. Vapor pressure profiles at the drum inlet.

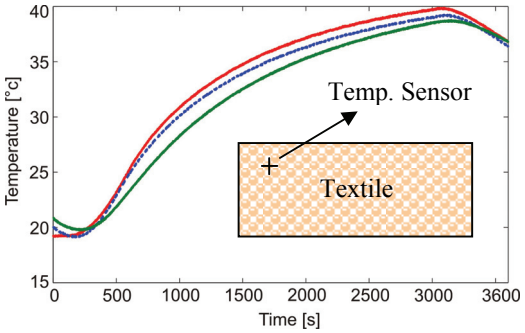


**Figure 6**. Measured textile temperature.

## Model A

The inputs to Model A are the inlet temperature and vapor pressure. The model simulation results are shown in figure 7. The error in the model is a consequence of the following resons:

1. The temperature sensor used has a diameter of 7mm and a length of 30mm. The model outputs a simulated temperature at a certain point, while the temperature sensor measures the temperature at many points along its surface and the output is an average.
2. The sensor used to measure the air relative humidity (for calculating the air vapor pressure) delivers false values once water drops condense on its surface.
3. The textile used in the tests has folds and the geometry is not uniform as in the simulation.
4. The air flow was not simulated in Model A.

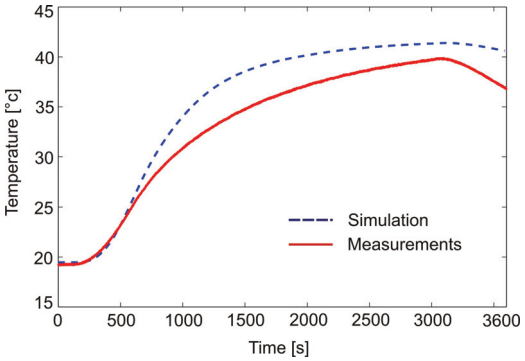


**Figure 7**. Comparison between the simulated and measured temperatures.

## Model B

Model B couples the air flow to the textile. Due to our limited computer power and the large drum area, we couldn't model the drum with the required mesh resolution. Therefore the drum size was reduced in the model and thus we didn't validate Model B results with the measurements. Still the results are comparable (Figure 8,9)

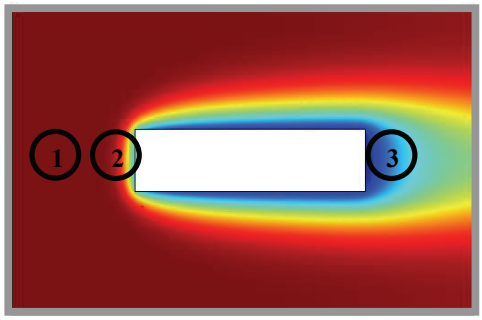


**Figure 8**. Air temperature profile along the drum after 1800 seconds.

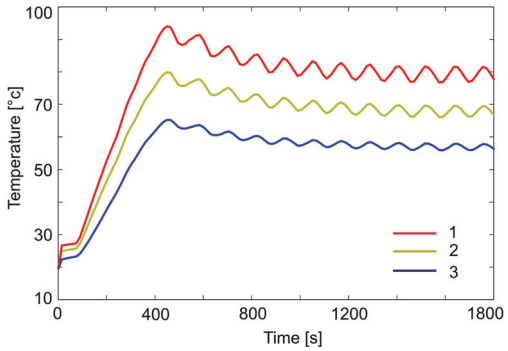


**Figure 9**. Temperature at the three points indicated in figure 8.

Once again the inputs to the model were the temperature (figure 4) and air moisture content/ vapor pressure (figure 5) at the inlet boundary (compare with equations 11, 12). Figure 9 shows that, the temperature at the textile boundaries (curves 2 and 3) is no longer equal to the inlet temperature (curve 1). It is lower, and that clarifies why the simulated temperature in figure 7 was higher than the measured. Since the air flow was not modeled in Model A, the inlet temperature was taken to be the boundary temperature which caused a false increase in the simulated textile temperature.

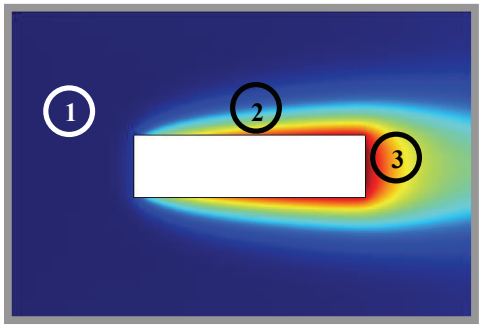


**Figure 10**. Air moisture content profile along the drum after 1800 seconds.

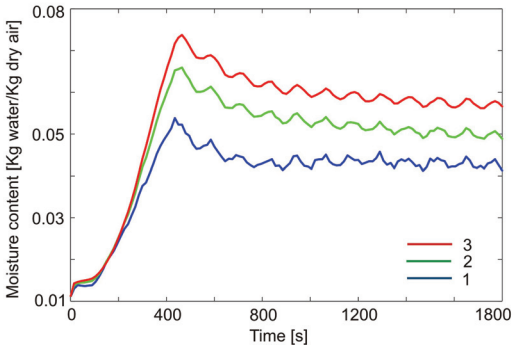


**Figure 11**. Moisture content at the three points indicated in figure10.

The peeks and sharp edges in curve 1, figure 11 are an indication that the integration step should be decreased. The integration step used for this simulation was 0.1 seconds. This supports our model enhancement proposal in the conclusion section.

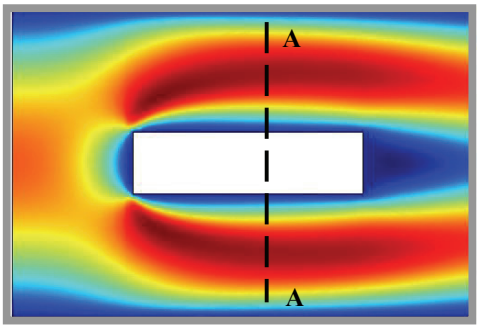


**Figure 12**. Air velocity profile along the drum after 1800 seconds.

In figure 4, as the hot dry air comes from the left, the left side of the textile dries faster. Curve 1 in figure 15 matches the ideal drying curve [4] where the three drying phases could be well identified. The constant drying phase ends at almost 300 seconds, then starts the first falling phase which lasts the most and ends around 1200 seconds. The third falling phase is characterized with rising temperatures and lasts as long as there is moisture in the textile.

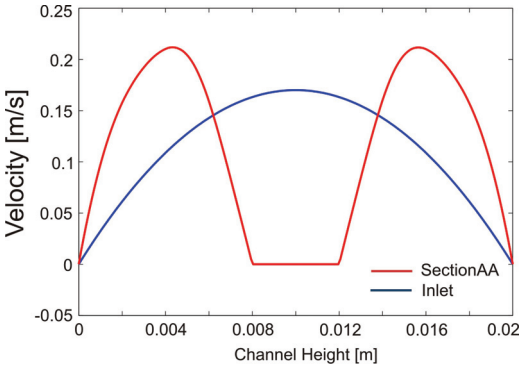


**Figure 13**. Velocity profile at the drum inlet and section AA demonstrated in figure 12.


**Figure 14**. Textile moisture content profile after 1800 seconds

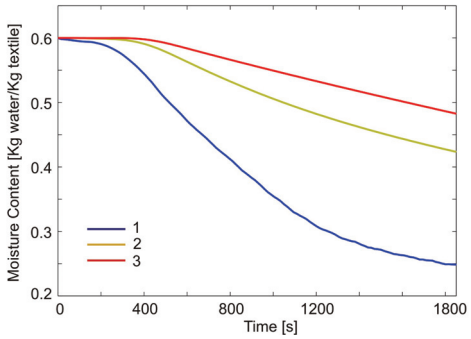


**Figure 15**. Textile moisture content profile at the three points indicated in figure 14

## 4. Conclusions

Two models were created using COMSOL Multiphysics to model energy, mass and momentum transport in textile and air during drying processes. Model A results show good agreement to the measurements where energy and mass transfer were successfully coupled on

one domain. In one way, the difference between simulation and measurements can be reduced by using a smaller thermocouple that has less surface area. We have also noticed that decreasing the integration step to 0.1 seconds improved the results and decreased the model error. So there is a tendency to further reduce the error in this direction.

Model B showed some interesting results where three conservation equations were coupled, not only on one domain, the model included coupling air and textile. Model B also helped in understanding the causes of the error in Model A. Unfortunately in such problems, modeling large areas needs high CPU power and memory capabilities.

## 5. References


1. P. Chen, D. Pei, A mathematical model of drying processes, *International Journal of Heat and Mass Transfer*, **32(2)**, 297-310 (1989)
2. F. Kneule, *Das Trocken*, Sauerlaender AG, Aarau (1975)
3. O. Krischer, *Die wissenschaftlichen Grundlagen der Trocknungstechnik*, Springer-Verlag, Berlin (1978)
4. A.V. Luikov, System of differential equation of heat and mass transfer in capillary porous bodies, *Int. J. Heat Mass Transfer*, **18**, 1-14 (1975)
5. S. Whitaker, Simultaneous heat and mass transfer in porous media: a theory of drying, *Advances in Heat Transfer*, **13**, 119-203 (1977)
6. Z. Zhang, S. Yang, D. Liu, Mechanism and Mathematical model of heat and mass transfer during convective drying of porous materials, *Heat Transfer-Asian Research*, **28(5)**, 337-351 (1999)